Cooperativity of two cavity-coupled qubits: a multi-partite-entanglement approach

Tian-tian Huan[1] and Hou Ian[1]

[1]*Institute of Applied Physics and Materials Engineering, FST, University of Macau, Macau*

Some nonlinear radiations such as superfluorescence can be understood as cooperative effects between atoms. We regard the cooperative radiation as a manifested effect secondary to the intrinsic cooperativity among the atoms and propose a time-resolved measure of cooperativity on a cavity-coupled dual-qubit system using multi-partite concurrence measures. We find that the cooperativity features a time delay characterisitic to superfluorescent pulses in its evolution, which coincides with the duration for the qubits to synchronize with each other. Thereafter, the cooperativity monotonically increases to a stationary value while the measure of asynchronicity dives to a steady minimum. Furthermore, the asynchronicity experiences a continuous transition to nonzero values when the coupling strength crosses from the weak to the strong coupling regime.

arXiv:1606.07209v1 [quant-ph] 23 Jun 2016

I. INTRODUCTION

The concept of cooperativity first appears in Dicke's famous formulation of superradiance [1], in which he quantified the cooperativity among N atoms through the eigenvalue of a collective angular momentum operator but did not question how each atom microscopically cooperates with its neighbors. Later, the theory of superfluorescence developed by Bonifacio [2] and others [3–5] capitulates Dicke's treatment and extends it to a full dynamic description. The former is a static perturbative approach to explain the cause of the amplified N^2 intensity of the collective spontaneous emission, whereas the latter derives the shape of the radiation in the form of a time-transient hyper-secant pulse from a Hamiltonian repleted with diplole interactions between each atom and a common multi-mode field. The pulse shape shows a concentrated amplitude rise and a reduced pulse duration compared to un-cooperated radiation, verifying the N^2 chacteristic of superradiance where the source energy from the atoms is conserved.

In addition to the pulse shape, the derivation about superfluorescence shows a characteristic delay in time between the initation of the radiation and the appearance of the pulse. Experimentally recorded on hydrofluoric gas [6], cesium [7], and most recently rubidium vapor [8], this delay shows the necessity of a finite time duration which the atoms use to cooperate themselves [9]. In theory, the delay is registered by the argument of the intensity of the hyper-secant pulse: the difference of time t from a characteristic time τ_D, i.e. the instantaneous intensity is maximal when t reaches τ_D [2].

The delay τ_D is proportional to both $\ln N$ and the relaxation time τ_R, but the product $\tau_R \ln N$ cannot serve as a cooperation quantifier for the atoms. It has been shown in molecular aggregates [10] that the atoms participate in cooperation only up to subgroups within the entire atomic ensemble when they demonstrate superradiance effect. In other words, not only is cooperated radiation feasible when the atoms are only partially participating in the cooperation, but cooperated lasing, i.e. superradiant laser, is also plausible when the participants are three-level atoms with lower levels being continuously driven [11, 12]. Such considerations lead one to distinguish the participants from the non-participants in the cooperated motions of a collective system. To this end, a static cooperativity measure has recently been proposed to count the cavity coupled to one shared resonator mode separately from the number of emitters coupled to their own resonator modes [13], the amount of which is believed to have direct consequences in the generation of nonclassical light [14]. Nonetheless, how a static cooperativity measure can be related to the studies in predicting the delay of a superfluorescent pulse is not yet explored.

More importantly, if one considers the cooperation among atomic systems as a dynamic process, time-independent integer measures are inadequate to determine if one particular atom initially not participating in the cooperation could join the cooperating process. Take a two-atom radiation system as an example. Using Dicke's method with the collective spin eigenvalue as an estimate, one can observe that an initial setup in the configuration $|\uparrow\uparrow\rangle$ or $|\downarrow\downarrow\rangle$ (using the spin notation for the atomic states) along the z-direction will result in minimal cooperation; whereas the configuration $|\uparrow\downarrow\rangle$ or $|\downarrow\uparrow\rangle$ would result in a maximal cooperation. But how does one determine the cooperativity if the initial state is a superposition of the four aforementioned configurations? Moreover, one cannot determine whether a two-atom system is minimally or maximally cooperated when its coupling to a common radiation field and to the environment might lead to a spin precession from, say, $|\uparrow\uparrow\rangle$ to $|\uparrow\downarrow\rangle$. A time-dependent measure is therefore required to resolve these concerns and we attempt to formulate a dynamic cooperativity in terms of entanglement measures.

Entanglement measures, such as negativity [15], concurrence [16], and their generalizations [17, 18], were originally proposed as measures in the real number domain to quantify the inseparability of static entangled states, such as the Bell states for bipartite systems, and the W-states and GHZ-states for multipartite systems. Recently, multiple studies have shown that entanglement plays an intimate role in the dynamics of optomechanical cavities [19–22]. Following this, we propose multipartite concurrences that maps on time-dependent density matrices as a measure of time-resolved microscopic cooperativity. We model the cooperativity on a circuit quantum electrodynamic (cQED) system [23] with two superconducting qubits entangled via their mutual coupling to the circuit cavity resonator, which readily displays the superradiance effect [24].

Using the arbitrary-dimension bipartite concurrence [18] on the two qubits and its generalization to tripartite concurrence for measuring the residual entanglement that distributes

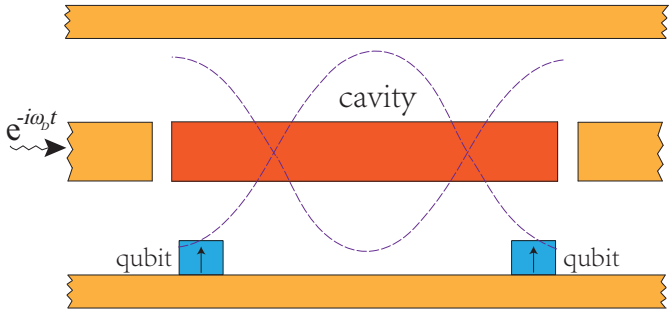

FIG. 1. (Color online) Schematic diagram of the proposed tripartite system: a cavity coupled two superconducting qubits on both sides acts as a transmission channel for microwave photons, which is the significant intermediary of the interaction between each two pair of subsystems. An external driving laser enters the cavity from the left side.

among the two qubits and the cavity resonator, we are able to identify a time delay in the initial evolution of the state vector with the cooperation time, after which the concurrence measures maximize to a stable value. When the eigenfrequencies of the two qubits are detuned, their asynchronization whose measures are extended from that of continuous variable systems [25] demonstrates identical signatures in its evolution, i.e. a time duration of the same length before it stabilizes to a minimum, showing the relation between cooperativity and synchronicity.

The article is organized as follows. We describe the model of the dressed dual-qubit circuit system and derive the evolution of its state vector in Sec. II. In Sec. III, we first simulate the system evolution, then explain the concurrence measures and apply them to the simulated results, and finally study their time characteristics by comparing them to the asynchronicity measure. Conclusions and discussions are given in Sec. IV.

II. DRESSED TRIPARTITE SYSTEM

As illustrated in Fig. 1, we consider a cQED system consisting of three parts: a cavity mode and two superconducting qubits, each of which is placed at the antinode of the two ends of the cavity resonator.

The total system Hamiltonian reads ($\hbar = 1$)

$$H = H_0 + H_{\rm int} + H_{\rm ext}, \tag{1}$$

$$H_0 = \omega_c a^\dagger a + \Omega_L \sigma_{L,z} + \Omega_R \sigma_{R,z}, \tag{2}$$

$$H_{\rm int} = \eta_L \left(a\sigma_{L,+} + a^\dagger \sigma_{L,-}\right) + \eta_R \left(a\sigma_{R,+} + a^\dagger \sigma_{R,-}\right) \tag{3}$$

$$H_{\rm ext} = i\varepsilon_D \left(a^\dagger e^{-i\omega_D t} - a e^{i\omega_D t}\right). \tag{4}$$

The part H_0 accounts for the free energy of the three parts, where ω_c denotes the frequency of the cavity mode and Ω_L (Ω_R) denotes the transition energy of the left (right) qubit, associated with the Pauli matrix $\sigma_{L,z}$ ($\sigma_{R,z}$). The part $H_{\rm int}$ accounts for the interactions between the cavity and each qubit under the JC-model with coupling strength η_L and η_R. The part $H_{\rm ext}$ accounts for the external driving field of eigenfrequency ω_D and Rabi frequency ε_D.

The combined system of a cavity and two qubits has its bare states described by the tensor product state $\{|e_L\rangle, |g_L\rangle\} \otimes \{|n\rangle\} \otimes \{|e_R\rangle, |g_R\rangle\}$, where $|e_L\rangle$ ($|g_L\rangle$) denotes the excited (ground) state of the left (right) qubit; $|n\rangle$ denotes the Fock number states of the cavity mode; $|e_R\rangle$ ($|g_R\rangle$) denotes the excited (ground) state of the right qubit. To simplifying the notation, we omit the subscripts L and R when writing the product states and let the first letter denote the state of the left qubit, the middle letter that of the cavity mode, and the last letter that of the right qubit (e.g. $|e, n, g\rangle = |e_L\rangle \otimes |n\rangle \otimes |g_R\rangle$).

The free Hamiltonian H_0 and the interaction Hamiltonian $H_{\rm int}$ constitute a closed subsystem, for which there exist dressed states that diagonalize $H_0 + H_{\rm int}$. To find an analytical expression for the dressed states, we consider the sets of energy-conserving states $|e, n, g\rangle$, $|g, n+1, g\rangle$, and $|g, n, e\rangle$, which are resonant within single-photon processes, to contribute to a dressed state for each n. In other words, the state $|e, n, e\rangle$ which is resonant with $|g, n+2, g\rangle$ through a double-photon process is avoided. These single-photon resonant states form an invariant subspace, for which the closed Hamiltonian consists of 3×3 symmetric block matrices. Therefore, we have the eigen-equation

$$(H_0 + H_{\rm int})\,|u_k^{(n)}\rangle = E_k^{(n)} \left|u_k^{(n)}\right\rangle, \tag{5}$$

where the eigenvectors $|u_k^{(n)}\rangle$ denote the dressed states that diagonalize the $3n \times 3n$ matrix $H_0 + H_{\rm int}$ and the eigenvalues $E_k^{(n)}$ denote the dressed-state energies in the diagonalized space. The index k enumerates $\{1, 2, 3\}$ to indicate the dressed levels within the n-th cluster.

Block-diagonalizing $H_0 + H_{\rm int}$ for Eq. (5) results in a cubic equation of $E_k^{(n)}$ for each n, whose roots are

$$E_k^{(n)} = \frac{2}{3}\sqrt{\delta_n^2 + 3(\Delta^2 + \eta_L^2 + \eta_R^2)}\cos\left(\theta + \frac{2k\pi}{3}\right) + \frac{\delta_n}{3}, \tag{6}$$

where the $\Delta = \Omega_L - \Omega_R$ denotes the left-right qubit detuning, $\delta_n = (n+1)\,\omega_c - \Omega_L - \Omega_R$ is the detuning between the cavity and the two qubits, and the angle is defined as

$$\theta = \frac{1}{3}\cos^{-1} 2\left(\delta_n^2 + 3\Delta^2 + 3(\eta_L^2 + \eta_R^2)\right)^{-3/2}\Big[2\delta_n^3 + 9\delta_n\left(\eta_L^2 + \eta_R^2\right) - 18\delta_n\Delta^2 + 27\Delta\left(\eta_L^2 - \eta_R^2\right)\Big]. \tag{7}$$

The corresponding eigenvector reads

$$|u_k^{(n)}\rangle = \alpha_{L,k}^{(n)}|e, n, g\rangle + \alpha_{C,k}^{(n)}|g, n+1, g\rangle + \alpha_{R,k}^{(n)}|g, n, e\rangle, \tag{8}$$

where the transformation coefficients are

$$\alpha_{L,k}^{(n)} = -\eta_L(\Delta + E_k^{(n)})\Big/ Z_k^{(n)}, \tag{9}$$

$$\alpha_{C,k}^{(n)} = \left[\Delta^2 - (E_k^{(n)})^2\right]\Big/ Z_k^{(n)}, \tag{10}$$

$$\alpha_{R,k}^{(n)} = \eta_R(\Delta - E_k^{(n)})\Big/ Z_k^{(n)}, \tag{11}$$

with $Z_k^{(n)}$ being the normalization constant

$$\left(Z_k^{(n)}\right)^2 = \eta_L^2\left[\Delta + E_k^{(n)}\right]^2 + \eta_R^2\left[\Delta - E_k^{(n)}\right]^2 + \left[\Delta^2 - (E_k^{(n)})^2\right]^2. \quad (12)$$

The derivation is given in the Appendix.

In the dressed space spanned by the basis vectors of Eq. (8), the closed Hamiltonian is written in the diagonalized form

$$H_0 + H_{\rm int} = \sum_{n,k} E_k^{(n)} |u_k^{(n)}\rangle\langle u_k^{(n)}|, \quad (13)$$

while the annihilation operator $a = \mathbb{I}_{\rm L} \otimes a \otimes \mathbb{I}_{\rm R} \approx \sum_n |g,n,e\rangle\langle g,n+1,e| + |e,n,g\rangle\langle e,n+1,g| + \sqrt{2}|g,n+1,g\rangle\langle g,n+2,g|$ under the single-photon processes is transformed to

$$a = \sum_{n,j,k}\Big[\alpha_{L,j}^{(n)*}\alpha_{L,k}^{(n+1)} + \sqrt{2}\alpha_{C,j}^{(n)*}\alpha_{C,k}^{(n+1)} + \alpha_{R,j}^{(n)*}\alpha_{R,k}^{(n+1)}\Big]|u_j^{(n)}\rangle\langle u_k^{(n+1)}|, \quad (14)$$

where the indices j and k enumerate over the set $\{1,2,3\}$.

The permitted dressed level transitions induced by the external driving can be found by substituting Eq. (14) into Eq. (4). In the weak-energy limit where the transitions are confined to the lowest two clusters of states ($n = 0$ and $n = 1$), the total Hamilitonian is written as

$$H^{(0,1)} = \sum_j\Big[E_j^{(0)}|u_j^{(0)}\rangle\langle u_j^{(0)}| + E_j^{(1)}|u_j^{(1)}\rangle\langle u_j^{(1)}|\Big] - \sum_{j,k} i\varepsilon_D e^{i\omega_D t}\Big[\Big(\alpha_{L,j}^{(0)*}\alpha_{L,k}^{(1)} + \sqrt{2}\alpha_{C,j}^{(0)*}\alpha_{C,k}^{(1)} + \alpha_{R,j}^{(0)*}\alpha_{R,k}^{(1)}\Big)|u_j^{(0)}\rangle\langle u_k^{(1)}| + \text{H.c.}\Big] \quad (15)$$

in the dressed space. Introducing the time-dependent state vector

$$|\psi(t)\rangle = \sum_j\Big(c_j(t)|u_j^{(0)}\rangle + d_j(t)|u_j^{(1)}\rangle\Big) \quad (16)$$

in the confined state space and applying it to the Hamiltonian above, one has the Schrödinger equations of the time coefficients

$$\dot{c}_j(t) = -iE_j^{(0)}c_j(t) - \varepsilon_D e^{i\omega_D t}\lambda_l\alpha_{l,j}^{(0)*}\alpha_{l,k}^{(1)}d_k(t), \quad (17)$$

$$\dot{d}_j(t) = -iE_j^{(1)}d_j(t) + \varepsilon_D e^{-i\omega_D t}\lambda_l\alpha_{l,j}^{(1)*}\alpha_{l,k}^{(0)}c_k(t), \quad (18)$$

where λ_l denotes the weight of the summation over the index l for the system component L (the left qubit), R (the right qubit), or C (the cavity), i.e. $\lambda_L = \lambda_R = 1$ and $\lambda_C = \sqrt{2}$. In the equations, we observe the Einstein summation convention.

In the rotating frame $c_j(t) = c_j'(t)\exp\{-iE_j^{(0)}t\}$ and $d_j(t) = d_j'(t)\exp\{-iE_j^{(1)}t\}$, the coupled equations can be written as the linear homogeneous system of differential equations $\dot{\mathbf{c}}' = A\mathbf{c}'$ where $\mathbf{c}' = [c_1'\ c_2'\ c_3'\ d_1'\ d_2'\ d_3']$ and

$$A = \begin{bmatrix} 0 & -\left[\varepsilon_D e^{i\zeta_{kj}t}\lambda_l\alpha_{l,j}^{(0)*}\alpha_{l,k}^{(1)}\right] \\ \left[\varepsilon_D e^{-i\zeta_{jk}t}\lambda_l\alpha_{l,j}^{(1)*}\alpha_{l,k}^{(0)}\right] & 0 \end{bmatrix}. \quad (19)$$

In the matrix A, we denote $\zeta_{kj} = \omega_D - \left(E_k^{(1)} - E_j^{(0)}\right)$ for the detuning between the driving and the dressed states. Since A is integrable, then solving the linear system for $\{c_j, d_j\}$ and expanding the dressed states by using the bare states in Eq. (16), one can find the expansion coefficients γ of the state vector

$$|\psi(t)\rangle = \gamma_L^{(0)}(t)|e,0,g\rangle + \gamma_C^{(0)}(t)|g,1,g\rangle + \gamma_R^{(0)}(t)|g,0,e\rangle + \gamma_L^{(1)}(t)|e,1,g\rangle + \gamma_C^{(1)}(t)|g,2,g\rangle + \gamma_R^{(1)}(t)|g,1,e\rangle \quad (20)$$

back in the bare state space.

III. COOPERATIVITY MEASURED BY ENTANGLEMENT

A. Evolution of the state vector

To see that the evolution of the state vector can initiate the cooperativity of the two delocalized qubits, we assume the cavity mode is initially driven by the external field to reach a partial population inversion while setting the qubits initially at the ground. In other words, the expansion coefficients at the initial moment are: $\gamma_C^{(0)} = \sqrt{0.9}$, $\gamma_L^{(1)} = \sqrt{0.1}$, and $\gamma_L^{(0)} = \gamma_R^{(0)} = \gamma_L^{(1)} = \gamma_R^{(1)} = 0$.

We simulate the evolutions of these coefficients in a C-program and plot them in Fig. 2, using the experimentally accessible parameters of superconducting charge qubits [26]: $\Omega_L/2\pi = \Omega_R/2\pi = 5.1$ GHz, $\eta_L/2\pi = \eta_R/2\pi = 300$ MHz, and $\omega_c/2\pi = 5.32$ GHz. The frequency of the external field is maintained at $\omega_D/2\pi = 5.3$ GHz while its driving strength retained at $\varepsilon_D/2\pi = 200$ KHz. The lower set of states with $n = 0$ is given in Fig. 2(a) whereas the upper set with $n = 1$ is given in Fig. 2(b).

We observe that for both the lower set and the upper set of states, there exists a transition point of the oscillations of the coefficients, which is located at about $4.5\ \mu$s in the plots. In particular, $\gamma_C^{(0)}$ is transited from a region of shrinking oscillation to a region of small fluctuation at this point. Meanwhile, $\gamma_L^{(1)}$,$\gamma_R^{(1)}$, and $\gamma_C^{(1)}$ are transited from an amplifying region to a region of saturated oscillation envelope. The contrasting behavior of the two sets of coefficients demonstrates that the energy excitation that exists in the cavity mode is transferred to the left and the right qubits whose complementary oscillations imply the build-up of the entanglement between them.

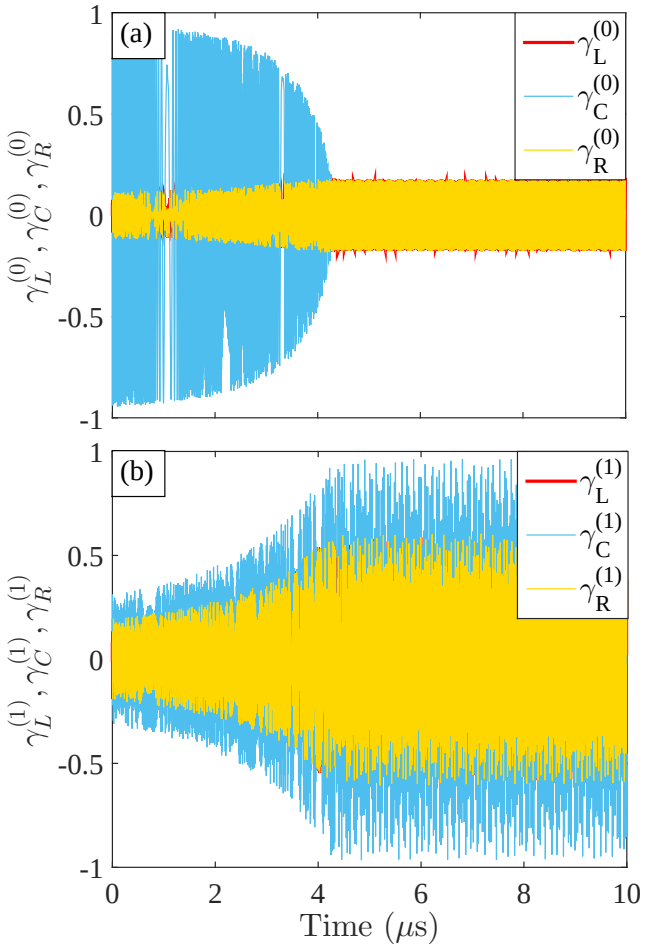

FIG. 2. (Color online) The time evolutions of the six expansion coefficients: (a) for $n = 0$; (b) for $n = 1$. The red, the blue, and the yellow curves associate with the state $|e, n, g\rangle$, $|g, n+1, g\rangle$, and $|g, n, e\rangle$, respectively.

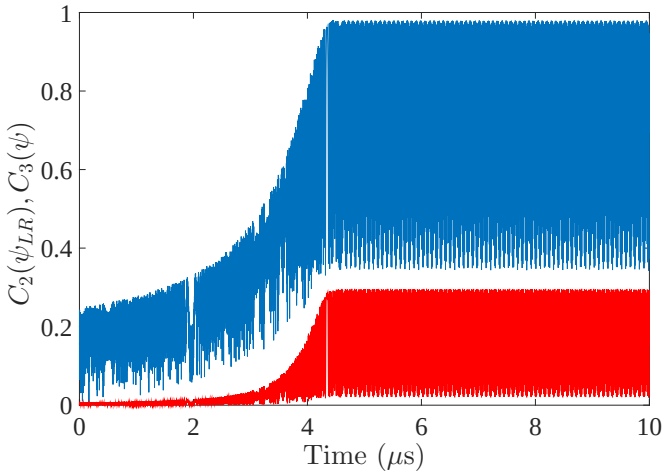

FIG. 3. (Color online) Time evolution of the bipartite concurrence $C_2\left(\psi_{LR}\right)$ between the two cavity-coupled qubits (blue) and the tripartite concurrence $C_3\left(\psi\right)$ among the qubits and the cavity (red). A symmetric scenario is assumed between the left and the right qubits: $\eta_L = \eta_R = 2\pi \times 300$ MHz and $\Omega_L = \Omega_R = 2\pi \times 5.1$ GHz.

B. Bipartite and tripartite concurrences

To fully capture the evolution characteristics of the two cavity-coupled qubits from a holistic point of view, we apply two entanglement measures – bipartite concurrence and tripartite concurrence – to the state vector of the total system.

The bipartite concurrence quantifies the inseparability of the joint pure state of two coupled systems of arbitrary dimensions by inverting the density matrix. For our case here, the joint state is the product state $|\psi_{LR}\rangle$ of the indirectly coupled left and right qubits. Thus the inversion is conducted through the superoperator $S_{D_1} \otimes S_{D_2}$ where the dimensions $D_1 = D_2 = 2$ and the bipartite concurrence is defined as $C_2(\psi_{LR}) = \sqrt{\langle\psi_{LR}|S_2 \otimes S_2\left(|\psi_{LR}\rangle\langle\psi_{LR}|\right)|\psi_{LR}\rangle}$. Given the consideration of pure states, for which $\mathrm{tr}\rho^2 = 1$ and $\mathrm{tr}\rho_L^2 = \mathrm{tr}\rho_R^2$, the definition reduces to $C_2(\psi_{LR}) = \sqrt{2\left[1 - \mathrm{tr}\left(\rho_L^2\right)\right]}$ where $\rho_L = \mathrm{tr}_R\left(\mathrm{tr}_C\left(|\psi\rangle\langle\psi|\right)\right)$ is the reduced density matrix of the left qubit.

Applying $|\psi\left(t\right)\rangle$ in Eq. (20) to the formula, we derive the evolution of the bipartite concurrence as illustrated in Fig. 3 by the blue curve. It becomes apparent that the transition point that manifests in Figs. 2(a) and 2(b) signifies the concurrence reaching a maximum after a gradual monotonic increase in the oscillation envelope. This maximum concurrence is retained thereafter. The finite delay time $\tau_D = 4.5$ μs that the concurrence spends to reach its maximal close-to-unit value reflects the time the two qubits spend on reaching a maximal cooperativity through their mutual couplings to the cavity mode, after which their cooperation would not recede.

The cavity mode plays an active part in initiating the entanglement between the two qubits. From the entanglement-theoretic point of view, the concurrence is distributed among the qubits as well as the cavity. Taking away the pairwise entanglements between any two parties in the tripartite system, one obtains the residual concurrence that remains as an equally distributed entanglement among all three parties [17]. Extending the original formulation on three-qubit systems, we generalize the inversion operations for two arbitray-dimensional systems given above to three arbitray-dimensional system. That is, we introduce the superoperator

$$\begin{aligned} S_{D_1} \otimes S_{D_2} \otimes S_{D_3}\left(\rho\right) = & I \otimes I \otimes I \\ & - I \otimes I \otimes \rho_R - \rho_L \otimes I \otimes I - I \otimes \rho_C \otimes I \\ & + \rho_{LR} \otimes I + I \otimes \rho_{CR} + \rho_{LC} \otimes I - \rho. \end{aligned} \quad (21)$$

for our $D_1 \times D_2 \times D_3$ dimension tripartite system, where $D_1 = D_3 = 2$ for the qubits and $D_2 = n$ for the cavity mode. In Eq. (21), I denotes the identity matrix while ρ_L, ρ_C, ρ_R, ρ_{LR}, ρ_{CR}, and ρ_{LC} denote the reduced density matrices of the components and the two-component subsystems. Applying the inversion, we thus derive a tripartite residual concurrence

$$C_3(\psi) = \sqrt{\langle\psi|S_{D_1}\otimes S_{D_2}\otimes S_{D_3}\left(|\psi\rangle\langle\psi|\right)|\psi\rangle}$$
$$= \left[1 - \mathrm{tr}\rho_R^2 - \mathrm{tr}\rho_L^2 - \mathrm{tr}\rho_C^2 + \mathrm{tr}\rho_{LR}^2 + \mathrm{tr}\rho_{CR}^2 + \mathrm{tr}\rho_{LC}^2 - \mathrm{tr}\rho^2\right]^{1/2}. \quad (22)$$

Again, using Eq. (20), we plot the tripartite concurrence as the red curve in Fig. 3. One can verify from the plot that the residual concurrence evolves in a similar fashion, which contains a signifying transition point at the exactly same location $\tau_D = 4.5$ μs as that of the bipartite concurrence. Before τ_D, it arises from a zero value under a similarly increasing envelope whereas, after τ_D, it retains a non-zero saturated value. The identical delay time again demonstrates the duration that the system components spend on cooperation before maximal cooperativity is reached.

Comparing Fig. 2 and Fig. 3, the energy quantum first dwells on the cavity mode ($|g,1,g\rangle$ and $|g,2,g\rangle$) without being emitted and absorbed by the qubits. Only when the two qubits start to establish a cooperated motion does the qubit-cavity-qubit resonance become effective such that the qubits be excited to their respective excited states $|e,1,g\rangle$ and $|g,1,e\rangle$. The entanglement is also established among the three components when the excitation takes off.

The concurrence measures plotted in Fig. 3 are computed upon a symmetric setting of system parameters: the level spacings and the coupling strengthes of the qubits are assumed identical. The tripartite concurrence of an asymmetric scenario with the right qubit level spacing raised to $\Omega_R/2\pi = 6.1$ GHz is shown as the green curve in Fig. 4 while the rest of the parameters remain unchanged. For comparison, the symmetric case is replotted as the red curve in the background. We observe that the delay to saturated cooperativity is inversely correlated with the eigen-frequency of either qubit, whichever has the higher one. For the plotted asymmetric case, the raised eigenfrequency of the right qubit reduces this delay time. On the other hand, symmetric settings lead to maximal cooperativity at saturation. The asymmetric case given by the green curve has the saturated cooperativity reduced to a lower level. Simulation under parameters set to various (not shown in figures) verify these observations.

The cooperativity between the qubits is also affected by how strong they are driven by the cavity mode, i.e. the coupling strengthes η_L and η_R. Shown in Fig. 5 for the symmetric scenario $\eta_L = \eta_R$, in general the greater the coupling, the less the delay τ_D, no matter the coupling is in the weak, strong, or ultra-strong regime. Meanwhile, the cooperativity reaches a higher saturated level accompanying a shorter delay time.

C. Cooperativity and synchronicity

Multi-partite concurrence as a measure of cooperativity reveals a gradual build-up of cooperation between two qubits in the time domain, explaining the existence of a delay in the superfluorescent pulse of cooperated radiation from a system-intrinsic point of view. This cooperativity is affected by many

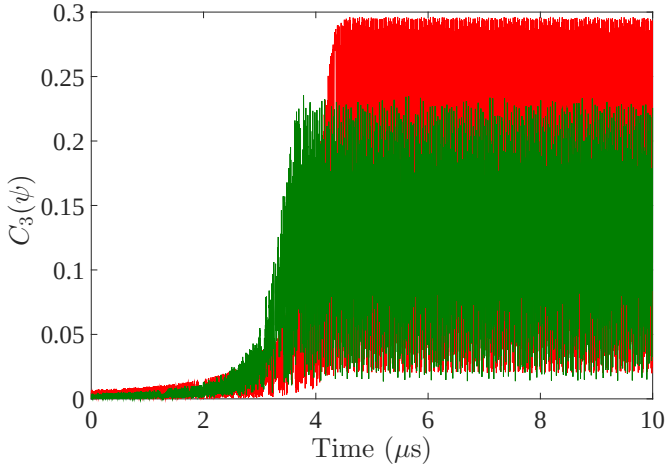

FIG. 4. (Color online) Comparison of the time evolutions of the tripartite concurrences between the symmetric (red curve) and the asymmetric (green curve) scenarios. For the symmetric case, both qubits are set to $\Omega_L/2\pi = \Omega_R/2\pi = 5.1$ GHz. For the asymmetric case, the right qubit is adjusted to $\Omega_R/2\pi = 6.1$ GHz. Coupling strengthes are retained at $\eta_L/2\pi = \eta_R/2\pi = 300$ MHz throughout.

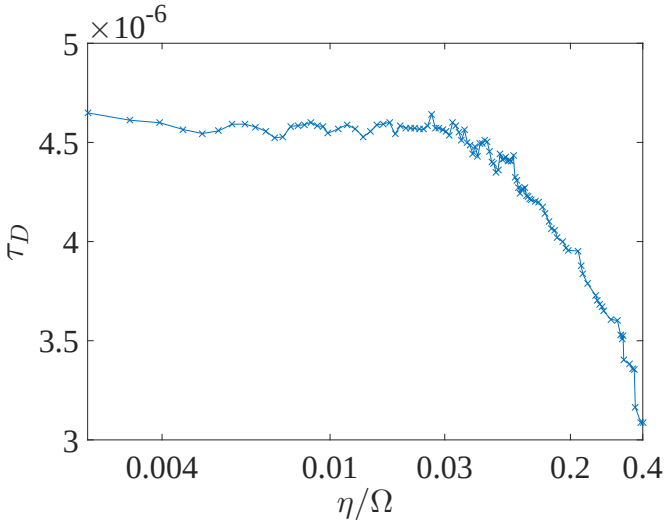

FIG. 5. The time delay τ_D is plotted as a function of the dimensionless coupling strength η/Ω in a semilog scale. Symmetric setting is assumed: the qubit level spacings $\Omega = \Omega_L = \Omega_R = 2\pi \times 5.1$ GHz, the coupling strength $\eta = \eta_L = \eta_R$. The crosses indicate the data points of the simulation runnings.

factors, among which the symmetry of the system parameters plays an important part. Tuning the system from a symmetric setting to an asymmetric setting is accompanied by tuning the transition rates of the qubits from a synchronous setting to an asynchronous setting. For the latter, we refer to the scenario where the population of the left qubit oscillates at a Rabi frequency not synchronous to that of the right qubit.

However, since two oscillators sharing a common oscillating platform are able to synchronize after certain time duration according to classical mechanics, we expect the qubits shar-

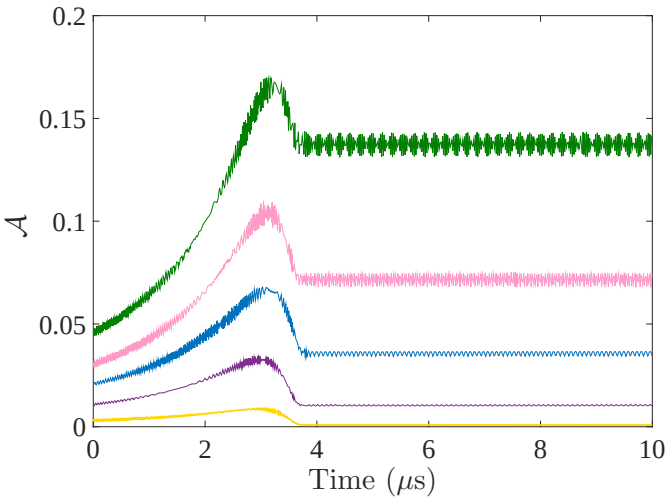

FIG. 6. (Color online) Asynchronization $\mathcal{A}$ of two cavity-coupled qubits under five different coupling strengthes: $\eta_L = \eta_R = 2\pi \times 50$ MHz (yellow), $2\pi \times 100$ MHz (purple), $2\pi \times 150$ MHz (blue), $2\pi \times 200$ MHz (pink), and $2\pi \times 300$ MHz (green). The qubit level spacings are kept at the asymmetric setting $\Omega_L/2\pi = 5.1$ GHz and $\Omega_R/2\pi = 6.1$ GHz.

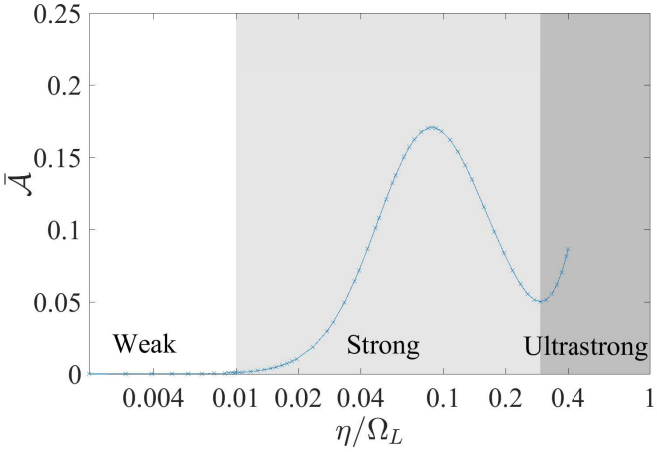

FIG. 7. The stable value $\bar{\mathcal{A}}$ is plotted as a function of the coupling strength $\eta = \eta_L = \eta_R$ in the logarithmic dimensionless scale of η/Ω_L, where the qubit level spacings are kept at the asymmetric setting $\Omega_L/2\pi = 5.1$ GHz and $\Omega_R/2\pi = 6.1$ GHz. The crosses indicate the data points of the simulation runnings.

ing the cavity resonator would behave similarly. To precisely describe the transition process from asynchronous regime to synchronous regime, we extend the quantum synchronization measure introduced recently by Mari et al. [25] for continuous variable systems to discrete systems. We consider instead the measure of asynchronicity

$$\mathcal{A}(t) = \Big|\det(\rho_L(t) - \rho_R(t))\Big|. \tag{23}$$

that compares the difference between two density matrices for two two-level systems.

When initiated from the cavity-driven initial state $|\psi(0)\rangle = 3|g,1,g\rangle/\sqrt{10}+|g,2,g\rangle/\sqrt{10}$, a symmetric setting $\Omega_L = \Omega_R$ would always lead to a zero asynchronicity throughout independent of the coupling strengthes η_L and η_R. When $\Omega_L \neq \Omega_R$, the asymmetry leads to coupling-dependent asynchronicity, as shown by the plots given in Fig. 6 for five settings of coupling strenghthes.

No matter the coupling strength, there exists a transition point after which the asynchronicity remains at a stable value. This transition point is identical to the transition point shown in Fig. 4 (green curves) where the tripartite concurrence reaches a maximal value. The coincidence verifies our expectation that the cooperativity is maximized when the asynchronicity is minimized. Therefore, cooperativity between two qubits reflects the dynamic identity of the two qubits.

Before reaching the stable minimal value, the asynchronicity increases from a non-zero value for a certain duration, which are spent on the cooperation by the qubits. When the coupling is sufficiently weak (below 50 MHz), the minimal stable value is almost vanishing (below 10^{-3}). When the coupling becomes stronger, the feedback from the cavity mode to each of the qubits becomes adverse to the synchronizing motion. However, the feedback effect is not linear. Plotted as a function of the dimensionless coupling strength η/Ω_L at $\Omega_L/2\pi = 5.1$ GHz and $\Omega_R/2\pi = 6.1$ GHz in Fig. 7, the stable minimal value $\bar{\mathcal{A}}$ of asynchronicity first retains a negligible value in the weak coupling regime. At about $\eta/\Omega_L = 0.01$, $\bar{\mathcal{A}}$ starts to increase until it reaches a maximum at $\eta/\Omega_L = 0.088$, where it starts to decrease until it reaches a minimum at $\eta/\Omega_L = 0.29$. The region between $\eta/\Omega_L = 0.01$ and $\eta/\Omega_L = 0.29$ can be regarded as a strong coupling regime for cooperativity. After that, $\bar{\mathcal{A}}$ enters the ultra-strong coupling regime and increases with the coupling again until $\eta/\Omega_L = 0.4$, where stable minimal value of $\mathcal{A}$ is no longer discernable.

IV. CONCLUSIONS AND DISCUSSIONS

We have solved the time evolution of a dressed circuit QED system comprising two qubits and a common cavity mode driven by an external microwave field. We propose a measure of cooperativity between the qubits using the tripartite residual concurrence measured on the three system components to interpret the time characteristics of the evolution, namely a transition point in the state vector coefficients. The concurrence shows a monotonic increase before the transition point and a saturated stable value after it. The two stages of evolutions coincide with the quantum asynchronicity between the density matrices of the qubits taking a pulsing shape and a stable minimal value, respectively. The delay before either the concurrence or the asynchronicity stabilizes is thus considered the time duration spent on cooperating by the indirectly coupled qubits, whose radiations into the common cavity mode would show a characterisitic delay according to the effect of superfluoresence.

Tripartite concurrence is a better measure than asynchronicity on quantifying cooperativity because, from the figures plotted, (i) asynchronicity vanishes when the qubits are set

identical while concurrence does not; (ii) the identity of the qubits maximizes the stable value of concurrence, reflecting one's intuition that symmetric settings in the system give rise to better cooperativity.

The charactistics of the evolution, including the delay and the value of the stablized asynchronicity, are highly dependent on the coupling strengthes of the qubits relative to the their level spacings. They demonstrate from the entanglement perspective the different behaviors that the circuit QED systems adopt when operating in weak, strong, and ultra-strong coupling regimes and illustrate, especially, the inadequacy of JC-model when dealing with evolution problems in the ultrastrong regime (e.g. the asynchronicity of Fig. 7).

The analysis presented is independent of the circuit geometry, in particular the cavity length. So the qubit entanglement could be realized on two delocalized qubits with a prolonged superconducting stripline resonator, providing an alternative scheme for quantum information transmission other than teleporting a pair of entangled photons.

ACKNOWLEDGMENTS

The authors thank the support by FDCT of Macau under grant 013/2013/A1, University of Macau under grants MRG022/IH/2013/FST and MYRG2014-00052-FST, and National Natural Science Foundation of China under grant No. 11404415.

APPENDIX: Solving the eigen-equation

From the eigen-equation Eq. (5), one has the determinant equation

$$\begin{vmatrix} \Delta - E^{(n)} & \eta_L & 0 \\ \eta_L & \delta_n - E^{(n)} & \eta_R \\ 0 & \eta_R & -\Delta - E^{(n)} \end{vmatrix} = 0 \qquad (24)$$

for each 3×3 block of the closed Hamiltonian $H_0 + H_{\rm int}$, where H_0 contributes the diagonal elements and $H_{\rm int}$ the off-diagonal elements.

This determinant equation is equivalent to the cubic equation

$$\left(E^{(n)}\right)^3 - \delta_n \left(E^{(n)}\right)^2 - \left(\Delta^2 + \eta_L^2 + \eta_R^2\right) E^{(n)} + \delta_n \Delta^2 - \Delta\left(\eta_L^2 - \eta_R^2\right) = 0 \qquad (25)$$

whose roots can be derived by absorbing the quadratic term through the transform $E^{(n)} = x + \frac{\delta_n}{3}$. The transformed equation becomes $x^3 + px + q = 0$, where

$$p = -\left(\frac{1}{3}\delta_n^2 + \Delta^2 + \eta_L^2 + \eta_R^2\right), \qquad (26)$$

$$q = -\frac{2}{27}\delta_n^3 - \frac{1}{3}\delta_n\left(\eta_L^2 + \eta_R^2\right) + \frac{2}{3}\delta_n\Delta^2 - \Delta\left(\eta_L^2 - \eta_R^2\right) \qquad (27)$$

In the close cavity-qubit resonance region $\delta_n \approx 0$, the discriminant D is simplified to

$$D = \frac{1}{4}\Delta^2\left(\eta_L - \eta_R\right)^4 - \frac{1}{27}\left(\Delta^2 + \eta_L^2 + \eta_R^2\right)^3. \qquad (28)$$

To let the cubic equation admit three non-degenerate real roots, we consider the range

$$\left(3 - 2\sqrt{2}\right)\eta_R < \eta_L < \left(3 + 2\sqrt{2}\right)\eta_R \qquad (29)$$

that makes $D < 0$, Applying the Vieta's formula, the roots x can be found with a parametric angle θ_n given by Eq. (7).

Using the eigenvalues given in Eq. (6) where k indexes the set of states within a cluster of given n and expanding the eigenvector $\left|u_k^{(n)}\right\rangle$ in the bare state space given by Eq. (8), we have the column matrix equation

$$\begin{bmatrix} \Delta - E_k^{(n)} & \eta_L & 0 \\ \eta_L & \delta_n - E_k^{(n)} & \eta_R \\ 0 & \eta_R & -\Delta - E_k^{(n)} \end{bmatrix} \begin{bmatrix} \alpha_{L,k}^{(n)} \\ \alpha_{C,k}^{(n)} \\ \alpha_{R,k}^{(n)} \end{bmatrix} = 0. \qquad (30)$$

Letting $\alpha_{C,k}^{(n)}$ be the proportional constant, we find $\alpha_{L,k}^{(n)} = -\eta_L \alpha_{C,k}^{(n)} \Big/ \left(\Delta - E_k^{(n)}\right)$ and $\alpha_{R,k}^{(n)} = \eta_R \alpha_{C,k}^{(n)} \Big/ \left(\Delta + E_k^{(n)}\right)$. Then normalizing the coefficients, their expressions are given by Eqs. (9) - (11).

[1] R. H. Dicke, Phys. Rev. **93**, 99 (1954).
[2] R. Bonifacio and L. A. Lugiato, Phys. Rev. A **11**, 1507 (1975); *ibid.* Phys. Rev. A **18**, 1129 (1978).
[3] R. Glauber and F. Haake, Phys. Lett. A **68**, 29 (1978).
[4] F. Haake, H. King, G. Schröder, J. Haus, R. Glauber, and F. Hopf, Phys. Rev. Lett. **42**, 1740 (1979).
[5] D. Polder, M. F. H. Schuurmans, and Q. H. F. Vrehen, Phys. Rev. A **19**, 1192 (1979).
[6] N. Skribanowitz, I. P. Herman, J. C. MacGillivray, and M. S. Feld, Phys. Rev. Lett. 30, 309 (1973).
[7] H. M. Gibbs, Q. H. F. Vrehen, and H. M. J. Hikspoors, Phys. Rev. Lett. **39**, 547 (1977).
[8] G. O. Ariunbold, M. M. Kash, V. A. Sautenkov, H. Li, Y. V. Rostovtsev, G. R. Welch, and M. O. Scully, Phys. Rev. A **82**, 043421 (2010).
[9] F. T. Arecchi and E. Courtens, Phys. Rev. A **2**, 1730 (1970).
[10] F. C. Spano and S. Mukamel, The Journal of Chemical Physics **91**, 683 (1989).
[11] F. Haake, M. I. Kolobov, C. Fabre, E. Giacobino, and S. Reynaud, Phys. Rev. Lett. **71**, 995 (1993).

[12] C. Seeger, M. I. Kolobov, M. Kuś, and F. Haake, Phys. Rev. A **54**, 4440 (1996).
[13] E. Mascarenhas, D. Gerace, M. F. Santos, and A. Auffèves, Phys. Rev. A **88**, 063825 (2013).
[14] D. Pagel, A. Alvermann, and H. Fehske, Phys. Rev. A **91**, 043814 (2015).
[15] G. Vidal and R. F. Werner, Phys. Rev. A **65**, 032314 (2002).
[16] W. K. Wootters, Phys. Rev. Lett. **80**, 2245 (1998).
[17] V. Coffman, J. Kundu, and W. K. Wootters, Phys. Rev. A **61**, 052306 (2000).
[18] P. Rungta, V. Buek, C. M. Caves, M. Hillery, and G. J. Milburn, Phys. Rev. A **64**, 042315 (2001).
[19] M. Abdi, S. Pirandola, P. Tombesi, and D. Vitali, Phys. Rev. Lett. **109**, 143601 (2012).
[20] L. Tian, Phys. Rev. Lett. **110**, 233602 (2013).
[21] Y.-D. Wang and A. A. Clerk, Phys. Rev. Lett. **110**, 253601 (2013).
[22] T. Huan, R. Zhou, and H. Ian, Phys. Rev. A **92**, 022301 (2015).
[23] A. Blais, R.-S. Huang, A. Wallraff, S. M. Girvin, and R. J. Schoelkopf, Phys. Rev. A **69**, 62320 (2004).
[24] J. A. Mlynek, A. A. Abdumalikov, C. Eichler, and A. Wallraff, Nat. Commun. **5**, 5186 (2014).
[25] A. Mari, A. Farace, N. Didier, V. Giovannetti, and R. Fazio, Phys. Rev. Lett. **111**, 103605 (2013).
[26] J. Majer, J. M. Chow, J. M. Gambetta, J. Koch, B. R. Johnson, J. A. Schreier, L. Frunzio, D. I. Schuster, A. A. Houck, A. Wallraff, A. Blais, M. H. Devoret, S. M. Girvin, and R. J. Schoelkopf, Nature **449**, 443 (2007).